Tetrahedron 65 (2009) 5521–5526

Contents lists available at ScienceDirect

Tetrahedron

journal homepage: www.elsevier.com/locate/tet

Effects of substituents and counterions on the structures of silenolates: a computational investigation

Anders M. Eklöf, Henrik Ottosson *

Department of Biochemistry and Organic Chemistry, Box 576, Uppsala University, 751 23 Uppsala, Sweden

ARTICLE INFO

Article history:
Received 22 January 2009
Received in revised form 7 February 2009
Accepted 8 February 2009
Available online 14 April 2009

ABSTRACT

The structures and charge distributions of substituted silenolates $[H_2SiC(=O)X]^-$ (X=H, SiH_3, Me, *t*-Bu, OMe, NMe_2; group **A**), $[Y_2SiC(=O)H]^-$ (Y=H, F, Me, Ph, SiH_3, $SiMe_3$; group **B**), and $[Y_2SiC(=O)X]^-$ (Y=Me, X=*t*-Bu, and Y=$SiMe_3$; X=*t*-Bu, OMe, NMe_2; group **C**) were examined through density functional theory calculations. The effects of the solvated counterion (K^+, Li^+, or $MgCl^+$) and coordination site (O or Si) on the properties of group **C** silenolates were also studied. The variation in the degree of π-conjugative reverse SiC bond polarization, $\Sigma\Phi_{RP}(\pi)$, calculated by natural resonance theory, was determined. The $\Sigma\Phi_{RP}(\pi)$ correlated with *r*(SiC) for both group **A** and **B** silenolates, and the correlation between $\Sigma\Phi_{RP}(\pi)$ and the sum of valence angles at Si, $\Sigma\alpha$(Si), was good for group **A** but poor for group **B** due to strong influence of the inductive effect. The SiC charge difference correlated well with $\Sigma\Phi_{RP}(\pi)$ for group **A**, but not for group **B**, again an effect of inductive substituent effects. The group **C** silenolates were coordinated to $Li(THF)_3^+$, $MgCl(THF)_4^+$, and $K(THF)_5^+$ either via the O or Si atom. The coordination energies show that coordination to the hard O is preferred for Li^+ and $MgCl^+$, but the K^+ ion coordinated simultaneously to Si and O. Coordination of the solvated metal ion to O resulted in shorter SiC bond length, an increased $\Sigma\alpha$(Si) value, and lower Δq(SiC) when compared to the naked silenolate. Choice of counterion and substituent provides a means to extensively vary the properties of silenolates such as their reactivity.

1. Introduction

While the chemistry of enolates has been thoroughly explored and also understood to a high degree,[1] the chemistry of their silicon analogs, silenolates (Scheme 1), has not. Studies of lithium silenolates were first reported by Biltueva and co-workers in 1989,[2] and later on, further studies were reported by Bravo-Zhivotovskii, Apeloig, Ohshita, and Ishikawa.[3–10] Ishikawa and co-workers in particular explored their reactions and found that while lithium silenolates with bulky alkyl or aryl substituents at carbon undergo rapid dimerization followed by degradation at ambient temperature, they are sufficiently stable at low temperature for characterization by NMR spectroscopy. A particularly interesting feature of lithium silenolates for their potential synthetic applications is their high selectivity for [4+2] cycloadditions in reactions with dienes.[5,7] This is in contrast to many other (formally) Si=C double bonded compounds, which often undergo competing [2+2] cycloaddition and ene reactions with dienes.[11] Indeed, a similarly high selectivity in reactions with dienes as silenolates display is found for neutral silenes that are strongly influenced by reversed Si=C bond polarization,[12,13] i.e., compounds with a $Si^{\delta-}=C^{\delta+}$ polarity rather than the natural $Si^{\delta+}=C^{\delta-}$ polarity.[14,15] Further studies of the properties of such species should be motivated by their potential applications in synthesis as they provide selective and efficient routes to silacyclohex-4-enes (Scheme 2). Such silacycles have been shown by Steel and co-workers to be useful starting points for further synthetic elaborations.[16]

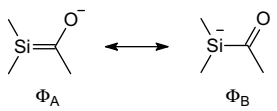

Scheme 1.

A few years ago, we formed the first isolable silenolate, $[(TMS)_2SiC(=O)t\text{-Bu}]^-K^+$ (TMS=$SiMe_3$), having a potassium instead of a lithium counterion, and characterized its structure by X-ray crystallography.[17] Surprisingly, we found that this potassium

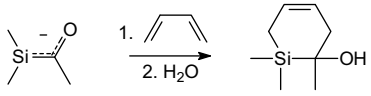

Scheme 2.

* Corresponding author.
E-mail address: henrik.ottosson@biorg.uu.se (H. Ottosson).

0040-4020/$ – see front matter © 2009 Elsevier Ltd. All rights reserved.
doi:10.1016/j.tet.2009.02.088

silenolate was stable in inert atmosphere at room temperature for up to three months, in contrast to the analogous lithium silenolates, which degraded within hours. X-ray crystal structure analysis revealed a SiC bond length of our potassium silenolate of 1.926 Å and the Si atom was markedly pyramidal with a sum of the valence angles ($\Sigma\alpha$(Si)) of 317.8°. The potassium cation was coordinated both to the Si atom and to the O atom with a slightly closer contact with the O atom. Calculations at B3LYP/6-31G(d) level of $[(H_3Si)_2SiC(=O)Me]^-K^+(OMe_2)_3$ gave a SiC bond length of 1.938 Å and a $\Sigma\alpha$(Si) of 307.0° in fair agreement with experiments.

It should be mentioned that only a few computational investigations have been performed on silenolates. Ohshita and co-workers calculated $[(H_3Si)_2SiC(=O)Me]^-$ at the HF/6-31G(d) level and found that the SiC bond length was 1.926 Å, close to that of a typical SiC single bond (1.87 Å[18]).[5] We previously performed B3LYP density functional theory (DFT) calculations on a large number of silenes, silenolates, and related compounds influenced by reverse SiC bond polarization.[15] It was found that the uncoordinated silenolates were best described by resonance structure Φ_B (Scheme 1), and that their Si centers were similar to those of silyl anions. On the other hand, Ishikawa and co-workers found through variable temperature ^{1}H NMR spectroscopy of the $[TMS_2SiC(=O)$-Mes]Li silenolate an activation energy for SiC bond rotation of 14.3 kcal/mol indicating partial Si=C double bond character.[5] It should therefore be important to explore how silenolate structure varies with counterion and with substituents, and if this property can be related to stability and reactivity.

The purpose of this study has been to investigate the degree of reverse polarization among selected silenolates that resemble those that have been studied experimentally, and to investigate how the structure of the silenolates depends on the degree of reverse polarization as influenced by substituents X and Y (Scheme 3). We calculate the contribution from reverse polarized resonance structures of type Φ_B using natural resonance theory (NRT) of Weinhold and co-workers.[19–21] In this way, we primarily measure the π-component of reverse SiC bond polarization, although the natural $Si^{\delta+}=C^{\delta-}$ polarization can also be lowered through inductive σ-donation from the substituents.[22]

We first discuss the three groups **A**–**C** of silenolates without any complexating metal ion (Scheme 2). Subsequently, we compare solvated lithium, potassium, and magnesium ions coordinated to group **C** silenolates in order to see how the counterion affects the geometry and charge distribution. For each counterion, we discuss two possible isomers; one where the counterion is bound to the O atom and one where it is bound to the Si atom. Our belief is that this fundamental study will show how to alter the properties of silenolates, ultimately providing guidance for formation of a series of silenolates.

A

X = H, Me, *t*Bu, OMe, NMe_2

B

Y = H, F, Me, Ph, SiH_3, TMS

C

X = *t*Bu; Y = Me, TMS
X = TMS; Y = OMe, NMe_2

Scheme 3.

2. Computational methods

Optimization of the silenolate geometries was made using the B3LYP hybrid density functional theory (DFT) method,[23] together with the 6-31G(d) basis set of Pople and Hariharan.[24] In order to verify that a true minimum on the potential energy surface (PES) had been reached, frequency calculations were performed at the same level of computation. Natural resonance theory (NRT)[19–21] calculations and natural population analysis (NPA)[25] calculations were performed in order to assess the degree of reverse polarization influence and the charge difference between the C atom and the Si atom, respectively. All calculations were performed using the Jaguar 5.5 program package,[26] except for the geometry optimizations of the complexes between the silenolates in group **C** and the solvated counterions, which were performed using the Gaussian 03 program package.[27]

3. Results and discussion

To assess the effect of the counterion on the structure of the silenolates, we first analyzed the structures and charge distributions of the uncoordinated silenolates.

3.1. Uncoordinated silenolates

All silenolates in group **A** have a contribution from π-conjugative reverse polarized resonance structures in the range 86.6–94.3% (Table 1), indicating that the uncoordinated silenolates should be regarded as acyl substituted silyl anions (resonance structure Φ_B) rather than silene-like species (resonance structure Φ_A). The optimized SiC bond lengths are 1.912–1.984 Å, significantly longer than a normal SiC single bond (1.87 Å),[18] and they have Si with pyramidalization angles ranging from 287.3 to 298.1°. It is clearly seen that increased influence of reverse polarization leads to longer SiC bond length and to smaller pyramidalization angles. The shortest SiC bond length is found for the silenolates with X=SiH_3 and the longest is found for the silenolates with X=NMe_2. These two silenolates also have the largest and smallest pyramidalization angles $\Sigma\alpha$(Si), respectively.

The charge difference Δq(SiC), i.e., the charge at C minus the charge at Si, ranges from −0.40 to 0.45 e. In most cases, particularly

Table 1
Contributions from reverse polarized resonance structures ($\Sigma\Phi_{RP}(\pi)$), selected geometrical parameters, and charge differences between the C and Si atoms of group **A** silenolates

$H_2SiC(=O)X$	$\Sigma\Phi_{RP}(\pi)$[a]	r(SiC)[b]	$\Sigma\alpha$(Si)[c]	Δq(SiC)[d]
X=H	90.5	1.927	293.9	−0.07
X=SiH_3	86.6	1.912	298.1	−0.35
X=TMS	87.3	1.917	298.0	−0.40
X=*t*-Bu	91.6	1.958	292.0	0.16
X=Me	92.1	1.948	292.2	0.15
X=OMe (conf. 1)[e]	92.8	1.972	288.6	0.45
X=OMe (conf. 2)[e]	94.0	1.960	287.7	0.41
X=NMe_2	94.3	1.984	287.3	0.35

[a] Total contribution, $\Sigma\Phi_{RP}(\pi)$, from all reverse polarized resonance structures, i.e., all resonance structures with a SiC single bond in percent.
[b] The SiC bond length in Å.
[c] The sum of the valence angles around Si in degrees.
[d] The charge difference between Si and C in electrons.
[e] In conformer 1, the OMe bond is *anti* to the C=O bond, while in conformer 2, the OMe bond is *syn* to the C=O bond.

Table 2
Contributions from reverse polarized resonance structure ($\Sigma\Phi_{RP(\pi)}$), selected geometric parameters, and charge differences between the C and Si atoms of group **B** silenolates

$Y_2SiC(=O)H$	$\Sigma\Phi_{RP(\pi)}$[a]	r(SiC)[b]	$\Sigma\alpha$(Si)[c]	Δq(SiC)[d]
Y=TMS	88.9	1.917	306.5	0.15
Y=Me	89.8	1.922	301.1	−0.71
Y=Ph	89.9	1.918	309.4	−0.80
Y=H	90.5	1.927	293.9	−0.07
$Y=SiH_3$	90.7	1.929	300.4	0.05
$Y=CF_3$	93.4	1.937	290.5	−0.55
Y=F	95.9	1.981	293.8	−1.06

[a] Total contribution from all reverse polarized resonance structures, i.e., all resonance structures with a SiC single bond in percent.
[b] The SiC bond length in Å.
[c] The sum of the valence angles around Si in degrees.
[d] The charge difference between Si and C in electrons.

for the most reverse polarized silenolates, the C instead of Si is the positive end of the SiC dipole, in line with the silenolates being very strongly reverse polarized. The silenolate with $X=SiMe_3$ has the lowest Δq(SiC) and one of the conformers of the silenolate with X=OMe has the highest. The correlation between $\Sigma\Phi_{RP}(\pi)$ and $\Sigma\alpha$(Si) is excellent (r^2=0.945), indicating that the pyramidalization angle around Si for group **A** silenolates primarily depends on the π-charge at Si and not very much on the differences in the inductive effect between the substituents at carbon. The correlation between $\Sigma\Phi_{RP}(\pi)$ and r(SiC) is also good (r^2=0.854), as is correlation between $\Sigma\Phi_{RP}(\pi)$ and Δq(SiC) (r^2=0.918). This reveals that for a set of silenolates that all have the same substituents at Si, it is the π-conjugative contribution of reverse polarization that determines the geometry and charge distribution of the SiC bond.

For the group **B** silenolates, the influence of reverse polarized resonance structures lies in range 88.9–95.9% (Table 2). The variation in $\Sigma\Phi_{RP}(\pi)$ is thus similar to that of group **A** silenolates, even though most of the substituents at Si do not affect the π-system explicitly. Yet, the most electronegative substituents stabilize the negative charge at Si, and resonance structures of type Φ_B become more dominant with these substituents. With the electropositive TMS substituents, the opposite effect can be found as seen when compared to the silenolate with Y=H, and that is also the situation with Y=Ph and Me. The SiC bonds are long for all silenolates in group **B** (1.917–1.981 Å) and the pyramidalization angles range from 290.5 to 306.5°.

Similar as for group **A** silenolates, a correlation exists between $\Sigma\Phi_{RP}(\pi)$ and r(SiC) (r^2=0.903). However, because the substituents at Si are varied in this group, a very poor correlation is found between $\Sigma\Phi_{RP}(\pi)$ and $\Sigma\alpha$(Si) (r^2=0.506), as the inductively withdrawing/donating ability of the substituents at Si will influence the structure around Si, similar as done in a silyl anion,[28] through the second-order Jahn–Teller effect (SOJT). The correlation between $\Sigma\Phi_{RP}(\pi)$ and Δq(SiC) is negligible (r^2=0.362), again indicating that q(Si) is strongly influenced by inductive effects of the substituents at Si and this effect is not to a similarly large extent reflected in $\Sigma\Phi_{RP}(\pi)$. It is noteworthy that whereas the TMS substituent leads to the group **B** silenolates with the least π-conjugative reverse polarization contribution, it gives the most reverse polarized charge distribution of the SiC bond. The opposite is the case with the fluoro substituent at Si, which leads to the silenolates with highest influence of reverse polarization. The SiC bond polarity clearly varies also with the electron donating and withdrawing ability of the substituents at Si. The variation of Δq(SiC) from −0.8 to 0.15 e shows that the positive end of the SiC dipole is on the Si atom in nearly all of these silenolates, a result of the fact that they in most cases have more inductively withdrawing substituents at Si when compared to group **A** silenolates with Y=H. Noteworthy is the large variation in Δq(SiC) that can be achieved through substitution as $-0.80<\Delta q(SiC)<0.45$ in groups **A** and **B** combined.

The corresponding data for the group **C** silenolates can be found in Tables 3–5. The degree of the π-conjugative reverse polarization ranges from 89.5 to 95.7%, the SiC bond lengths are found within 1.947–1.978 Å, and the pyramidalization angle around Si varies within 298.7–312.6°, i.e., in similar ranges as found for groups **A** and **B** silenolates. The correlation between $\Sigma\Phi_{RP}(\pi)$ and both r(SiC) (r^2=0.544) and $\Sigma\alpha$(Si) (r^2=0.727) are poor and there is no correlation between $\Sigma\Phi_{RP}(\pi)$ and Δq(SiC) (r^2=0.321), revealing that the inductive effect is also strongly influencing the charge distribution in the SiC bond, in addition to the π-conjugative reverse polarization effect.

3.2. Coordinated silenolates

Before discussing the effect of the counterion on r(SiC), $\Sigma\alpha$(Si), and Δq(SiC) of the silenolates in group **C**, we compare our calculated structure of $[TMS_2SiC(=O)t\text{-Bu}]K(THF)_5$ with the crystal structure published by us earlier, i.e., the same potassium silenolate with the potassium ion coordinated to [18]-crown-6-ether,[17] in order to validate our results. We found that if more than five THF solvent molecules around the K^+ ion were included in the calculation, one of them drifted away during the optimization. The numbers of THF molecules around the Li and Mg ions were determined in the same way, and the proper numbers of THF molecules around these metal silenolates are three and four, respectively. It is noteworthy that the potassium ion is closer to the O atom than to the Si atom in both our calculated structure and in the crystal structure. The calculated SiC bond length of 1.939 Å is in good agreement with the one from the crystallographic data (1.926 Å) and the same holds for the pyramidalization angle (317.4° in the calculated structure vs 317.8° in the crystal structure). This indicates that B3LYP/6-31G(d) describes the geometries of the silenolates studied here reasonably well.

In the present computational study, two isomers were found for the lithium and magnesium silenolates, one where the metal ion was coordinated to the O atom of the silenolate and one where it was coordinated to the Si atom. For the potassium silenolates, these two isomers were found to collapse into a single isomer, where the potassium ion was coordinated to both the O and the Si atom, consistent with the larger size of the potassium ion. The two isomers of $[TMS_2SiC(=O)t\text{-Bu}]Li(THF)_3$, the two isomers of $[TMS_2SiC(=O)t\text{-Bu}]MgCl(THF)_4$, and the one isomer of $[TMS_2SiC(=O)t\text{-Bu}]K(THF)_5$ are shown in Figure 1. The larger solvent shell around the K^+ ion is of special interest since this indeed could be one of the reasons for the higher thermal stability of potassium

Table 3
The SiC bond lengths (Å) of group **C** silenolates listed for the different counterions and coordination sites[a]

	M^1=:, M^2=:	M^1=Li, M^2=:	M^1=:, M^2=Li	M^1=MgCl, M^2=:	M^1=:, M^2=MgCl	M^1=K, M^2=:
$TMS_2Si(M^2)C(=OM^1)t\text{-Bu}$	1.954	1.879	1.966	1.852	1.983	1.939
$Me_2Si(M^2)C(=OM^1)t\text{-Bu}$	1.958	1.879	1.965	1.851	1.974	1.941
$TMS_2Si(M^2)C(=OM^1)OMe$ (conformer 1)[b]	1.947	1.934	1.946	1.913	1.952	1.947
$TMS_2Si(M^2)C(=OM^1)OMe$ (conformer 2)[b]	1.978	1.926	1.966	1.912	1.972	1.945
$TMS_2Si(M^2)C(=OM^1)NMe_2$	1.992	1.983	1.977	1.948	1.979	1.994

[a] M^1 and M^2 represent either a metal or an electron pair, where an electron pair is indicated by ':'.
[b] In conformer 1, the O–Me bond is *anti* to the C=O bond, whereas in conformer 2 the O–Me bond is *syn* to the C=O bond.

Table 4
Sum of valence angles at Si ($\Sigma\alpha$(Si)) of the group **C** silenolates listed for the different counterions and coordination sites[a]

	M^1=:, M^2=:	M^1=Li, M^2=:	M^1=:, M^2=Li	M^1=MgCl, M^2=:	M^1=:, M^2=MgCl	M^1=K, M^2=:
$TMS_2Si(M^2)C(=OM^1)t$-Bu	312.6	333.2	317.1	351.7	314.4	321.7
$Me_2Si(M^2)C(=OM^1)t$-Bu	300.2	322.7	310.7	330.7	310.1	309.2
$TMS_2Si(M^2)C(=OM^1)$OMe (conformer 1)[b]	302.1	308.2	309.6	314.2	306.5	304.4
$TMS_2Si(M^2)C(=OM^1)$OMe (conformer 2)[b]	298.7	311.9	311.3	324.6	315.9	317.4
$TMS_2Si(M^2)C(=OM^1)NMe_2$	296.3	317.5	312.8	316.8	314.8	317.4

[a] M^1 and M^2 represent either a metal or an electron pair, where an electron pair is indicated by ':'.
[b] In conformer 1, the O–Me bond is *anti* to the C=O bond whereas in conformer 2, the O–Me bond is *syn* to the C=O bond.

silenolates in an inert atmosphere as compared to lithium silenolates (vide infra). As will be shown below, lithium silenolates have more Si=C double bond character than the potassium silenolates due to stronger coordination, and they should therefore have more silene-type reactivity,[11] for example, be more prone to dimerize.

The maximum change in SiC bond length due to the change of metal ion and site of coordination was 0.10 Å (Table 3), and the maximum change in pyramidalization angle was 40° (Table 4). It is also found that the change of substituents at Si from methyl groups to TMS groups affects the SiC bond length very little (0.010 Å). For both the lithium and magnesium silenolates with a *tert*-butyl substituent at C, it can be seen that when the metal ion is coordinated to the O atom, the SiC bond is significantly shorter than the SiC bond in the naked silenolate. Clearly, the positively charged counterion raises the effective electronegativity of the O atom and increases the influence of resonance structures of type Φ_A (Scheme 1). This effect is also more pronounced for magnesium than for the lithium silenolates since the MgO bond should have a higher degree of covalent character than the LiO bond, and thus Mg lowers the π-donating ability of the O atom more. By increasing the M–O covalent bond strength one will eventually reach a Brook-type silene with M as SiR_3. Indeed, this hints to a gradual change in SiC double bond character as one goes from a free silenolates to a Brook-type silene.

When the metal ion is coordinated to the Si atom of the same silenolate, the opposite effect is seen and the SiC bond lengthens when compared to the naked silenolate. This is because the influence of resonance structures of type Φ_B is now increased instead, and the species should properly be described as metal coordinated silyl anions with acyl substituents. Again, the effect is more pronounced for magnesium silenolates because of a presumably stronger covalent character of the MgSi bond than of the LiSi bond.

For the silenolates substituted with π-donating OMe or NMe_2 groups at C, a slightly different behavior is observed. The deviation in bond length due to the counterion and site of coordination is now between 0.03 and 0.07 Å, compared to 0.10 Å for the *tert*-butyl substituted silenolates. When the metal ion was coordinated to the O atom of the silenolate, a shorter SiC bond length compared to that of the naked silenolate was observed, perfectly in line with what was seen for the alkyl-substituted silenolates. However, when the metal ion is coordinated to the Si atom of the silenolate, the SiC bond length is also shorter, or in one case somewhat longer, than that of the naked silenolate, in contrast to what was observed for the *tert*-butyl substituted silenolates. It should be noted that the maximum SiC bond length deviation due to changing the counterion in the *tert*-butyl substituted silenolates was larger when the counterion was coordinated to the O atom (0.10 Å) compared to when the counterion was coordinated to the Si atom (0.03 Å). For the potassium silenolates, the SiC bond length is always slightly shorter or approximately equal to the SiC bond length in the uncoordinated silenolate, consistent with the fact that the K^+ ion always was slightly closer to the O atom than to the Si atom.

The $\Sigma\alpha$(Si) was found to be larger when the counterion is coordinated to the O atom than what it is for the naked silenolates (Table 4), consistent with the shorter SiC bond in the *O*-metalated silenolates. This effect is also more pronounced for the magnesium silenolates than for the lithium silenolates, and shows on the gradual transformation between a free silenolate and a Brook-type silene as the covalent M–O bond character increases. It could also be seen that $\Sigma\alpha$(Si) is larger when the counterion is coordinated to the Si atom than in the uncoordinated silenolate. For the Si coordinated metal silenolates, $\Sigma\alpha$(Si) is raised by a lower amount when $M=MgCl^+$ than when $M=Li^+$, in line with the longer SiC bonds of the magnesium silenolates when compared with the corresponding lithium silenolates. Moreover, the degree of pyramidalization becomes smaller when TMS substituents are present at Si instead of methyl substituents, in line with the larger steric bulk of the former substituents. Finally, the potassium silenolates have a smaller degree of pyramidalization around Si than in the corresponding naked silenolates, and $\Sigma\alpha$(Si) lies between that of the lithium and magnesium silenolates.

A metal ion coordinated to the Si atom of the silenolate will stabilize a negative charge at this atom, and thus we expect Δq(SiC) to be larger for these lithium and magnesium silenolate isomers when compared to the corresponding naked silenolates. This was also the case (Table 5). In contrast, when the metal ion is coordinated to the O atom of the silenolate, the effective electronegativity of the O atom is raised and this causes Δq(SiC) to decrease when compared to the corresponding naked silenolate. Note that none of these changes mentioned above cause Δq(SiC) to change sign. It is also clear that the Δq(SiC) is larger for the lithium ester silenolates than for the corresponding lithium *tert*-butyl silenolates (Table 5). This is in line with the observations by Ohshita and co-workers, which indicate that the anionic charge is more localized on Si in lithium ester silenolates than what it is in alkyl-substituted lithium silenolates.[8] They also concluded that lithium ester silenolates, in contrast to alkyl-substituted silenolates give no *O*-silylated products upon reaction with Et_3SiCl.[5] For the potassium

Table 5
The SiC charge difference, Δq(SiC), in *e* of the group **C** silenolates listed for each of the different counterions and coordination sites[a]

	M^1=:, M^2=:	M^1=Li, M^2=:	M^1=:, M^2=Li	M^1=MgCl, M^2=:	M^1=:, M^2=MgCl	M^1=K, M^2=:
$TMS_2Si(M^2)C(=OM^1)t$-Bu	0.39	0.18	0.63	0.04	0.66	0.45
$Me_2Si(M^2)C(=OM^1)t$-Bu	−0.48	−0.81	−0.39	−0.96	−0.37	−0.52
$TMS_2Si(M^2)C(=OM^1)$OMe (conf. 1)[b]	0.64	0.68	0.84	0.58	0.87	0.73
$TMS_2Si(M^2)C(=OM^1)$OMe (conf. 2)[b]	0.74	0.63	0.90	0.57	0.91	0.71
$TMS_2Si(M^2)C(=OM^1)ONMe_2$	0.62	0.60	0.77	0.52	0.75	0.66

[a] M^1 and M^2 represent either a metal or an electron pair where an electron pair is indicated by ':'.
[b] In conformer 1, the O–Me bond is *anti* to the C=O bond, whereas in conformer 2, the O–Me bond is *syn* to the C=O bond.

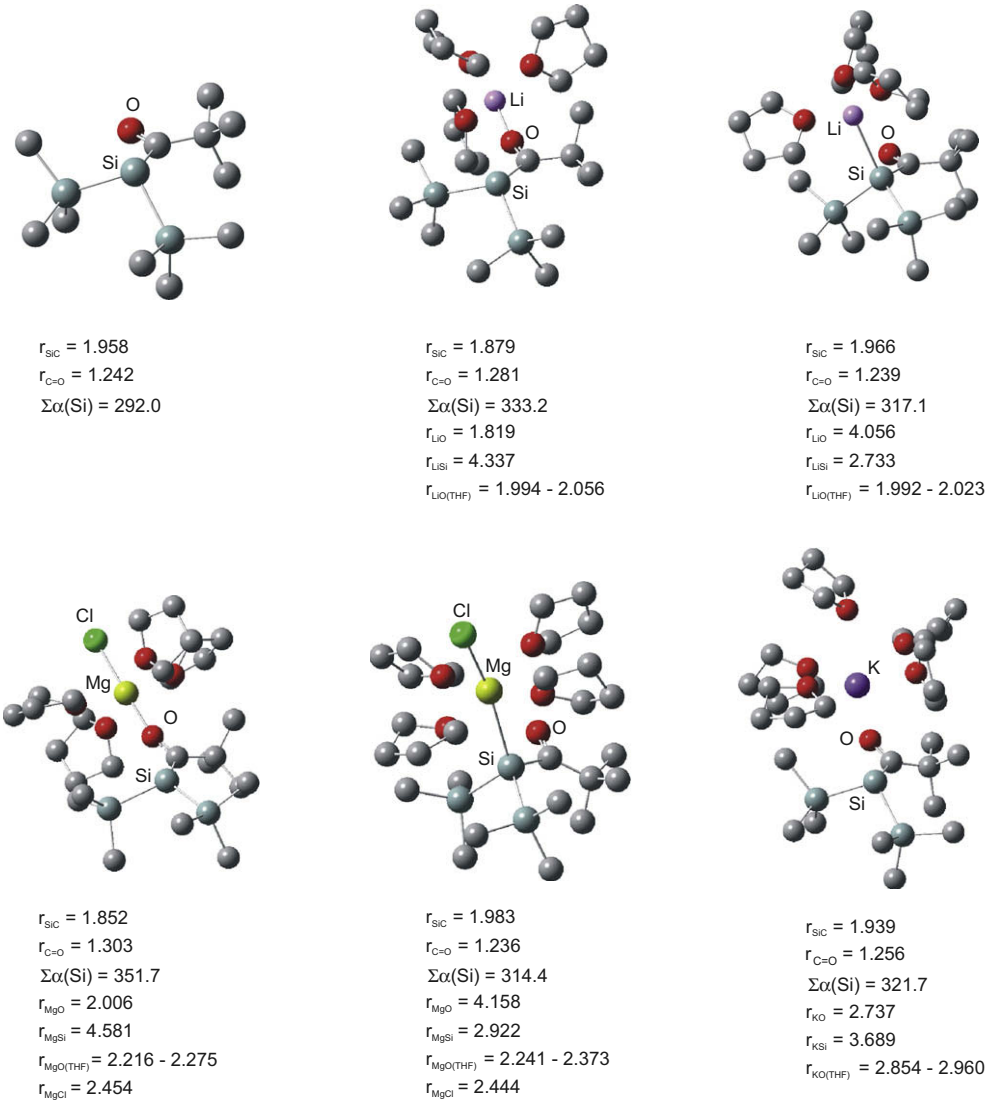

Figure 1. Optimal B3LYP/6-31G(d) geometries of $(TMS)_2SiC(=O)t$-Bu, $(TMS)_2SiC(=O)t$-BuLi$(THF)_3$ with Li coordinated to O, $(TMS)_2SiC(=O)t$-BuLi$(THF)_3$ with Li coordinated to Si, $(TMS)_2SiC(=O)t$-BuMgCl$(THF)_4$ with Mg coordinated to O, $(TMS)_2SiC(=O)t$-BuMgCl$(THF)_4$ with Mg coordinated to Si, and $(TMS)_2SiC(=O)t$-BuK$(THF)_5$ with K coordinated to both O and Si. Hydrogen atoms omitted for clarity. Distances in Å and angles in degrees.

silenolates, a largest deviation of only 0.09 e in Δq(SiC) when compared to the corresponding naked silenolate was observed, and this is consistent with the potassium ion coordinating to both the O and Si atoms of the silenolate. Finally, it is seen that the negative end of the SiC dipole is on Si for the silenolates with TMS substituents at Si and on C for the silenolates with methyl substituents at Si in line with earlier findings.[22]

The energies of the different metal ion coordinated silenolates relative to the naked silenolates and the free solvated metal ion are found in Table 6. For the lithium and magnesium silenolates, coordination to the harder O is preferred over coordination to the softer Si. Since the SiC bond lengths of the group **C** silenolates where the solvated lithium ion is coordinated to O is shorter than in the naked silenolates, this result is in line with the NMR investigations by Ohshita and co-workers on lithium silenolates and lithium ester silenolates, which show that the central SiC bond in these species possesses some double bond character.[5,8] For each of the silenolates the solvated potassium ion gives the weakest coordination, the solvated Li^+ or $MgCl^+$ ions having association energies that are higher by 7–17 kcal/mol. The isolability of the potassium silenolates could thus ultimately stem from the larger solvent shell around the potassium ion, and as a consequence, the

Table 6
The association energies of the different metal ion coordinated silenolates in kcal/mol relative to the naked silenolates and free solvated metal ion[a]

	M^1=Li, M^2=:	M^1=:, M^2=Li	M^1=MgCl, M^2=:	M^1=:, M^2=MgCl	M^1=K, M^2=:
$TMS_2Si(M^2)C(=OM^1)t$-Bu	−83.4	−79.1	−76.3	−68.5	−68.6
$Me_2Si(M^2)C(=OM^1)t$-Bu	−95.3	−89.4	−92.1	−88.5	−79.5
$TMS_2Si(M^2)C(=OM^1)$OMe (conformer 1)[b]	−83.5	−82.1	−79.0	−73.0	−70.2
$TMS_2Si(M^2)C(=OM^1)$OMe (conformer 2)[b]	−89.4	−79.4	−88.7	−67.5	−72.4
$TMS_2Si(M^2)C(=OM^1)NMe_2$	−86.2	−79.4	−77.5	−70.6	−70.4

[a] M^1 and M^2 represent either a metal or an electron pair where an electron pair is indicated by ':'.
[b] In conformer 1, the OMe bond is *anti* to the C=O bond, whereas in conformer 2, the OMe bond is *syn* to the C=O bond.

weaker coordination of K^+ to the silenolates. Because of the weaker binding, the potassium silenolates are nearly fully represented by resonance structure Φ_A (Scheme 1), and they have very little silene character (Φ_B). They will therefore be less prone to decompose through silene-type chemistry such as dimerization. One could thus postulate that by adding a strong Li^+ complexating agent, the thermal stability of lithium silenolates could possibly also be increased.

4. Conclusions

All silenolates studied were found to be highly influenced by reverse polarization (≥86%) due to the negatively charged O atom being a very strong π-electron donor and the higher bond strength of the C=O π-bond than of the Si=C π-bond. The correlations between the degree of reverse polarization influence and the SiC bond lengths of the group **A** and group **B** silenolates were found to be reasonable (r^2=0.854 and r^2=0.903, respectively). The pyramidalization angle around Si also correlated well with the degree of reverse polarization influence for the silenolates in group **A** (r^2=0.945), and this indicates that for a set of silenolates with the same substituents at Si, both r(SiC) and $\Sigma\alpha$(Si) are determined by the π-conjugative reverse polarization effect.

The lithium or magnesium ion prefers coordination to the hard O site of the silenolates, and shorter bond lengths and less pyramidal structure at Si result for the *tert*-butyl substituted group **C** silenolates due to increased influence of resonance structures of type Φ_A. For the potassium silenolate, it was found that the K^+ ion coordinated simultaneously to the O and Si atoms of the silenolate with a slightly closer coordination to O. In most cases, the SiC bond lengths shortened modestly when a group **C** silenolate was coordinated to a potassium ion. The pyramidalization angles around Si in the potassium silenolates increase in all cases, similar as they do for the lithium and magnesium silenolates.

The coordination energies of the metal ion coordinated silenolates indicate that coordination of the solvated metal ion to O is preferred over coordination to Si. The most stable lithium silenolate isomers thus have shorter SiC bond than the corresponding potassium silenolates. Furthermore, lithium silenolates react more as silenes than potassium silenolates, e.g., the lithium silenolates should be more prone to dimerize than the potassium silenolates. Indeed, the possibility to alter the structure of silenolates through choice of counterion should provide for a possibility to alter the reactivity of silenolates between the silene and silyl anion end points represented by the Φ_A and Φ_B resonance structures.

Acknowledgements

The authors wish to thank the Swedish Research Council for financial support and the National Supercomputer Center (NSC) for the most generous allotment of computer time.

References and notes

1. Caine, D. *Comprehensive Organic Synthesis*; Pergamon: Oxford, 1991; Vol. 3, Chapter 1.1.
2. Biltueva, I. S.; Bravo-Zhivotovskii, D. A.; Kalikhman, I. D.; Vitovskii, V. Yu.; Shevchenko, S. G.; Vyazankin, N. S.; Voronkov, M. G. *J. Organomet. Chem.* **1989**, *368*, 163.
3. Bravo-Zhivotovskii, D. A.; Apeloig, Y.; Ovchinnikov, Y.; Igonin, V.; Struchkov, Y. T. *J. Organomet. Chem.* **1993**, *446*, 123.
4. Ohshita, J.; Masaoka, Y.; Masaoka, S.; Ishikawa, M.; Tachibana, A.; Yano, T.; Yamabe, T. *J. Organomet. Chem.* **1994**, *473*, 15.
5. Ohshita, J.; Masaoka, Y.; Masaoka, S.; Hasebe, M.; Ishikawa, M.; Tachibana, A.; Yano, T.; Yamabe, T. *Organometallics* **1996**, *15*, 3136.
6. Ohshita, J.; Masaoka, S.; Ishikawa, M. *Organometallics* **1996**, *15*, 2198.
7. Ohshita, J.; Masaoka, S.; Morimoto, Y.; Sano, M.; Ishikawa, M. *Organmetallics* **1997**, *16*, 1123.
8. Ohshita, J.; Sakurai, H.; Tokunaga, Y.; Kunai, A. *Organometallics* **1999**, *18*, 4545.
9. Ohshita, J.; Sakurai, H.; Masaoka, S.; Tamai, M.; Kunai, A.; Ishikawa, M. *J. Organomet. Chem.* **2001**, *633*, 131.
10. Ohshita, J.; Tamai, M.; Sakurai, H.; Kunai, A. *Organometallics* **2001**, *20*, 1065.
11. For recent reviews on multiply bonded Si compounds see, e.g. (a) Brook, A. G.; Brook, M. A. *Adv. Organomet. Chem.* **1996**, *36*, 71; (b) Müller, T.; Ziche, W.; Auner, N. In *The Chemistry of Organic Silicon Compounds*; Rappoport, Z., Apeloig, Y., Eds.; Wiley Interscience: New York, NY, 1998; Vol. 2, p 857; (c) West, R. *J. Organomet. Chem.* **2001**, *21*, 467; (d) Gusel'nikov, L. E. *Coord. Chem. Rev.* **2003**, *244*, 149; (e) Ottosson, H.; Steel, P. G. *Chem.—Eur. J.* **2006**, *12*, 1576; (f) Ottosson, H.; Eklöf, A. M. *Coord. Chem. Rev.* **2008**, *252*, 1287.
12. Sakamoto, K.; Ogasawara, J.; Sakurai, H.; Kira, M. *J. Am. Chem. Soc.* **1997**, *119*, 3405.
13. El-Sayed, I.; Guliashvili, T.; Hazell, R.; Gogoll, A.; Ottosson, H. *Org. Lett.* **2002**, *4*, 1915.
14. Apeloig, Y.; Karni, M. *J. Am. Chem. Soc.* **1984**, *106*, 6676.
15. Ottosson, H. *Chem.—Eur. J.* **2003**, *9*, 4144.
16. (a) Berry, M. B.; Griffiths, R. J.; Sanganee, M. J.; Steel, P. G.; Whelligan, D. K. *Tetrahedron Lett.* **2003**, *44*, 9135; (b) Berry, M. B.; Griffiths, R. J.; Sanganee, M. J.; Steel, P. G.; Whelligan, D. K. *Org. Biomol. Chem.* **2004**, *2*, 2381; (c) Sellars, J. D.; Steel, P. G.; Turner, M. J. *Chem. Commun.* **2006**, 2385; (d) Sellars, J. D.; Steel, P. G. *Org. Biomol. Chem.* **2006**, *4*, 3223.
17. Guliashvili, T.; El-Sayed, I.; Fischer, A.; Ottosson, H. *Angew. Chem., Int. Ed.* **2003**, *42*, 1640.
18. Kaftory, M.; Kapon, M.; Botoshansky, M. In *The Chemistry of Organosilicon Compounds*; Rappoport, Z., Apeloig, Y., Eds.; Wiley: Chichester, UK, 1998; Vol. 2, p 181.
19. Glendening, E. D.; Weinhold, F. *J. Comput. Chem.* **1998**, *19*, 593.
20. Glendening, E. D.; Weinhold, F. *J. Comput. Chem.* **1998**, *19*, 610.
21. Glendening, E. D.; Badenhoop, J. K.; Weinhold, F. *J. Comput. Chem.* **1998**, *19*, 628.
22. Bendikov, M.; Quadt, S. R.; Rabin, O.; Apeloig, Y. *J. Am. Chem. Soc.* **2002**, *21*, 3930.
23. Becke, A. D. *J. Chem. Phys.* **1993**, *98*, 5648.
24. Hariharan, P. C.; Pople, J. A. *Theor. Chim. Acta* **1973**, *28*, 213.
25. Reed, A. E.; Weinstock, R. B.; Weinhold, F. *J. Chem. Phys.* **1985**, *83*, 735.
26. *Jaguar 5.5*; Schrodinger, LLC: Portland, Oregon, 2003.
27. Frisch, M. J.; Trucks, G. W.; Schlegel, H. B.; Scuseria, G. E.; Robb, M. A.; Cheeseman, J. R.; Montgomery, J. A., Jr.; Vreven, T.; Kudin, K. N.; Burant, J. C.; Millam, J. M.; Iyengar, S. S.; Tomasi, J.; Barone, V.; Mennucci, B.; Cossi, M.; Scalmani, G.; Rega, N.; Petersson, G. A.; Nakatsuji, H.; Hada, M.; Ehara, M.; Toyota, K.; Fukuda, R.; Hasegawa, J.; Ishida, M.; Nakajima, T.; Honda, Y.; Kitao, O.; Nakai, H.; Klene, M.; Li, X.; Knox, J. E.; Hratchian, H. P.; Cross, J. B.; Bakken, V.; Adamo, C.; Jaramillo, J.; Gomperts, R.; Stratmann, R. E.; Yazyev, O.; Austin, A. J.; Cammi, R.; Pomelli, C.; Ochterski, J. W.; Ayala, P. Y.; Morokuma, K.; Voth, G. A.; Salvador, P.; Dannenberg, J. J.; Zakrzewski, V. G.; Dapprich, S.; Daniels, A. D.; Strain, M. C.; Farkas, O.; Malick, D. K.; Rabuck, A. D.; Raghavachari, K.; Foresman, J. B.; Ortiz, J. V.; Cui, Q.; Baboul, A. G.; Clifford, S.; Cioslowski, J.; Stefanov, B. B.; Liu, G.; Liashenko, A.; Piskorz, P.; Komaromi, I.; Martin, R. L.; Fox, D. J.; Keith, T.; Al-Laham, M. A.; Peng, C. Y.; Nanayakkara, A.; Challacombe, M.; Gill, P. M. W.; Johnson, B.; Chen, W.; Wong, M. W.; Gonzalez, C.; Pople, J. A. *Gaussian 03, Revision D.01*; Gaussian: Wallingford CT, 2004.
28. Flock, M.; Marschner, C. *Chem.—Eur. J.* **2005**, *11*, 4635.